



Advances in Diffusion Barrier Coatings for High-Temperature Applications

Toshio Narita¹ · Yasumichi Kato¹ · Takuro Narita¹ · Mayumi Ara¹

Received: 7 August 2023 / Revised: 24 September 2023 / Accepted: 25 September 2023 /
Published online: 2 November 2023
© The Author(s) 2023

Abstract

Diffusion barrier coating (DBC) systems on heat resistant alloys consist of a multi-layer structure: an outer Al-reservoir layer and an inner diffusion barrier layer (DBL). The outer Al-reservoir layer forms a protective Al_2O_3 scale and DBL acts as a barrier layer against alloy interdiffusion. Three kinds of DBL were developed: Re on Ni-based superalloys; W on stainless steels; and Cr on Ni–Cr alloys. It was found that DBC systems have excellent mechanical properties (creep and fatigue), improving alloy substrate performance, and enhance the anti-exfoliation properties of YSZ in thermal barrier coatings (TBC) in addition to providing excellent oxidation resistance. At temperatures higher than 1300 °C, however, the DBC design based on kinetics (diffusion) is insufficient to form and maintain a protective Al_2O_3 scale. In this case a self-maintaining coating (SMC) system designed on the basis of thermodynamics (phase stability) is required. The SMC system formed on Nb–Hf (C-103) alloy consists of a multi-layer structure: an outer Re (Al, Si)_{1.8} and inner NbSi₂ layers, plus a transient Nb₅Si₃ layers formed during oxidation. At temperatures higher than 1300 °C the Al_2O_3 can be formed by changing the Al/Si ratio in the Re (Al, Si)_{1.8} in which Si was supplied from the decomposition reaction of NbSi₂ to Si + Nb₅Si₃ during selective oxidation of Al. It is proposed that coating alloys should be designed for considering not only high temperature oxidation, but also alloy substrate mechanical properties and anti-exfoliation of oxide scales, based on both kinetic principles (DBC system) and thermodynamics (SMC system).

Keywords High temperature oxidation · Diffusion barrier coating system · Self-maintaining coating system · Creep · Fatigue

✉ Toshio Narita
dbc@dbcsystem.co.jp

¹ DBC System R&D Co., Ltd., 1-515-3, Zenibako, Otaru-City, Hokkaido 047-0261, Japan

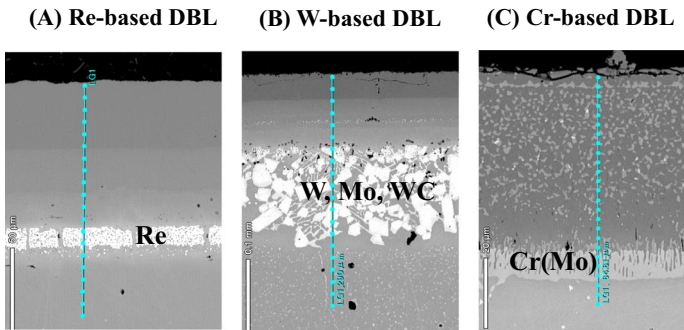
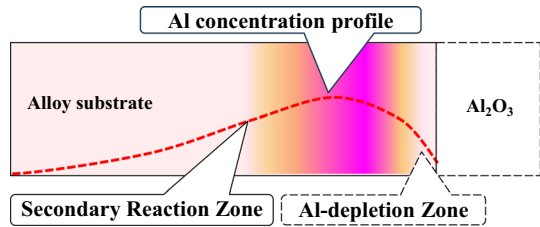


Fig. 1 Microstructures of three types of DBC systems. **A** σ -Re(Cr, Ni), **B** W-(Mo, WC) based alloys, and **C** α -Cr(Mo)

Fig. 2 Degradation of the coating layer structure



DBC System Defined

A diffusion barrier coating (DBC) system [1, 2] should provide excellent high-temperature oxidation resistance [3, 4] and can improve the mechanical properties (creep and fatigue) of the base material [5] and the peeling resistance of the YSZ layer of the thermal barrier coating (TBC) [6]. In this paper, we introduce the recent progress of the DBC [7] and SMC systems developed by authors at the DBC System R&D Co., Ltd. The results presented in this paper have not been published.

Formation of a DBC System

As shown in Fig. 1, three types of DBL were formed by a combination of electroplating or slurry coating, heat treatment, and Al diffusion treatment [8–11]. The Re (Cr–Ni) based barrier layer can be precisely controlled in thickness, and is formed onto a Ni-based single crystal superalloy. A relatively thick W (Mo, WC)-based barrier layer can be formed, making it suitable for general-purpose substrates such as stainless steels. The Cr (Mo) barrier layer is a α -Cr phase that is naturally formed when Al diffusion treatment was carried out on Ni–Cr-based alloys containing about 20 at% or more Cr.

Conventional Coatings and DBC Systems

Conventional coatings have an Al-containing alloy layer formed on the surface of the alloy substrates by making use of electroplating, thermal spraying, and EBPVD or the like. At high temperatures, as shown in Fig. 2, an aluminum depletion zone is formed under the Al_2O_3 film by selective oxidation of aluminum. Further, interdiffusion occurs between the coating layer and the alloy substrate, and the secondary reaction zone (SRZ) develops. The formation of the Al-depletion zone and the SRZ causes degradation of the oxidation resistance of the coating film. Furthermore, in a case of the Ni-based single crystal superalloy the formation of the SRZ causes reduction in the creep rupture times of the base material as will be described later.

The diffusion barrier coating (DBC) system proposed by the authors [1, 2] has a structure in which a diffusion barrier layer is inserted between the alloy substrate and the Al-containing layer, as shown in Fig. 3. This DBL inserted has a function of suppressing the mutual diffusion of elements between the base material and the Al-containing layer. From the viewpoint of diffusion suppression, refractory metals (W, Re, Mo, Nb, Ta, Cr) are candidate elements for the diffusion barrier layer.

Ni-Based Single Crystal Superalloys

SRZ

Thermal barrier coating (TBC; bond coat of MCrAlY and top-coat of YSZ) was formed on Ni-based single crystal superalloy by using thermal spraying (HVOF and Plasma), and then an oxidation test was performed at 1050 °C for 1000 h in air. It was found that interdiffusion between the alloy substrate and the bond coat MCrAlY proceeds significantly, resulting in poly-crystallization of the single crystal structure about 80 μm depth, as shown in Fig. 4a, in which Electron Backscatter Diffraction (EBSD) method was adopted to reveal micro-crystal structures.

A Re-based DBL with about 20 μm in thickness was formed on a single crystal superalloy and then the same TBC as those shown in Fig. 4a was over-coated. The DBC/TBC coated superalloy was oxidized under the same conditions as those in Fig. 4a. Re-crystallization of about 10 μm thickness was observed as a sort of SRZ in Fig. 4b between the Re-based DBL and alloy substrate. The SRZ of the DBC/TBC is significantly suppressed in contrast to that of conventional TBC.

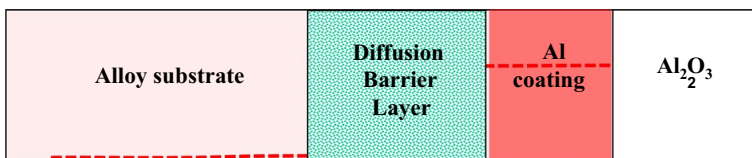


Fig. 3 Schematics of DBC system with DBL and Al-reservoir layer

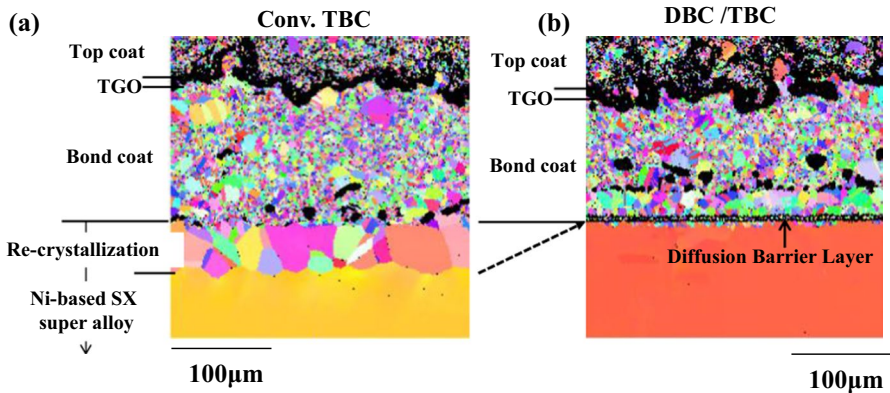
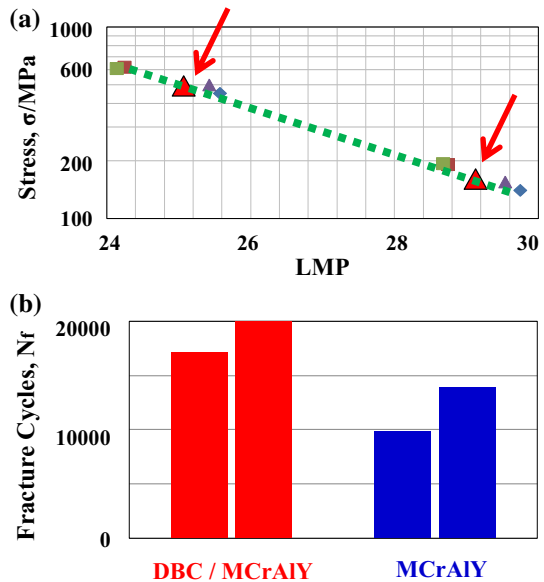


Fig. 4 a Conventional TBC, b DBC/TBC

Fig. 5 a Creep (LMP-plot) of Ni-based single crystal superalloy with and without DBC/TBC, b Fracture cycles of Ni-based single crystal superalloy with DBC/MCrAlY or MCrAlY



Creep and Fatigue

The creep and fatigue characteristics of Ni-based single crystal superalloys coated with and without DBC/TBC were investigated. When the stress of the creep test is plotted by the Larson Mirror Parameter (LMP), as shown in Fig. 5a two points (red arrows 920 °C/450 MPa and 1040 °C/140 MPa) for the DBC/TBC were on a straight line of the data of the alloy substrate. The decrease in creep rupture times with a DBC/TBC was scarcely observed.

Fatigue tests at 920 °C, (strain rate: 0.4%/s, full strain 0.7%, tri-angle wave, exposure at 1050 °C for 100 h) showed that the number of rupture cycles of DBC/MCrAlY increased by about twice as high as that of the MCrAlY coating, as shown in Fig. 5b. It is concluded that the DBC system is effective in improving fatigue properties.

Cyclic Oxidation

Cyclic oxidation tests (1093 °C; 10 h \leftrightarrow RT in air, DSS) of a Ni-based single crystal superalloy with DBC/TBC were performed. For comparison, the results of the thermal cycling test of the superalloy with conventional TBC are also given.

As shown in Fig. 6, it was revealed that the YSZ of the top coat layer of conventional TBC was completely peeled off at 126 cycles, while the peeling rate of the YSZ layer of DBC/TBC was lower than 20% of total surface area after 300 cycles. It can be seen that for Ni-based single crystal superalloys the exfoliation resistance of the YSZ layer of TBC is greatly improved by the DBL.

Ni-Based Alloy (Hastelloy-X)

Figure 7 shows creep curves obtained for a Ni-based alloy (HX; Hastelloy X) with or without a Re-based DBL/ β -NiAl coating. Creep conditions are as follows: temperature 970 °C; stresses 40, 27.5 and 22.5 MPa. It was found at 27.5 MPa that the creep rupture time of the HX alloy with DBC is about twice as that of the bare alloy.

In the creep test at a stress of 22.5 MPa, the test was interrupted at 3% strain (creep time 180 h). As shown in Fig. 8, the Re-based DBL is uniformly creep-deformed over the entire surface of the test specimen, and cracks are not observed.

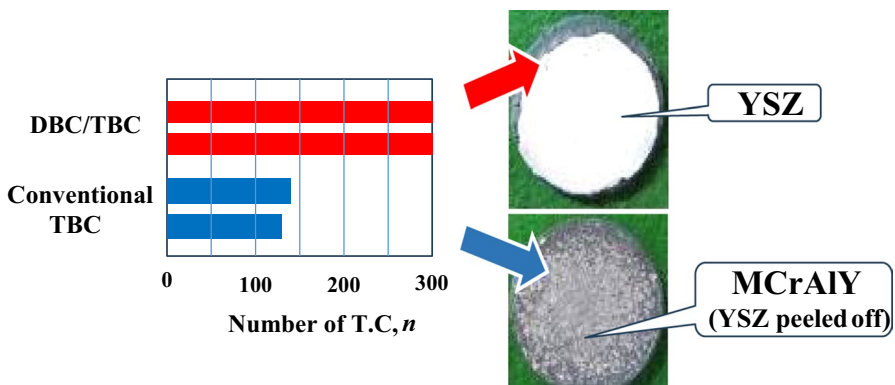


Fig. 6 Top-views of DBC/TBC and the conventional TBC after thermal cyclic tests

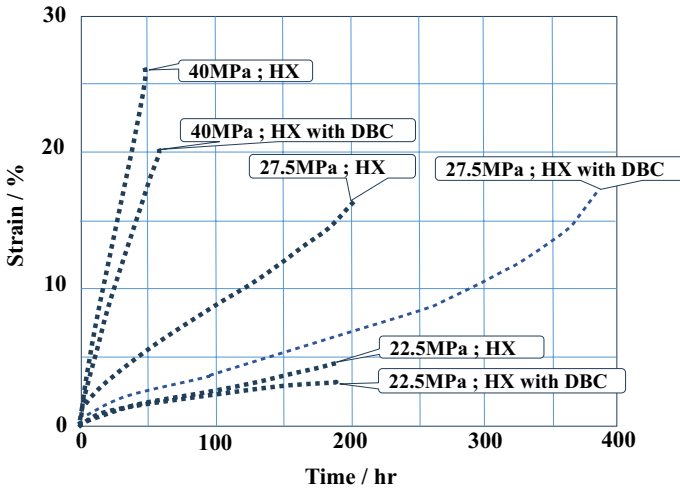
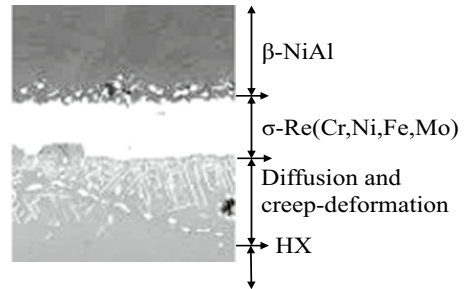


Fig. 7 Creep curves of HX with and without DBC (β -NiAl)

Fig. 8 Cross-sectional micro-structure of HX with DBC after a creep test (22.5 MPa and strain 3% for 180 h)



From these results, it is presumed that the σ phase (Re–Cr–Ni) constituting the DBL can be creep-deformed due to the fact that the alloy elements and their concentrations of the DBL differ from the σ phase of the single-crystal superalloy, which is well-known to be the harmful mechanical phase. More detailed research will be conducted in the future.

Fe-Based Alloy (SUS310S)

Figure 9a shows the creep curves of Fe–25Cr–20Ni alloy (SUS310S) with or without a Re-based DBL/ β -NiAl coating. A creep test was carried out under the following conditions: temperature 900 °C; stress 22.5 MPa in air. Creep deformation of SUS310S

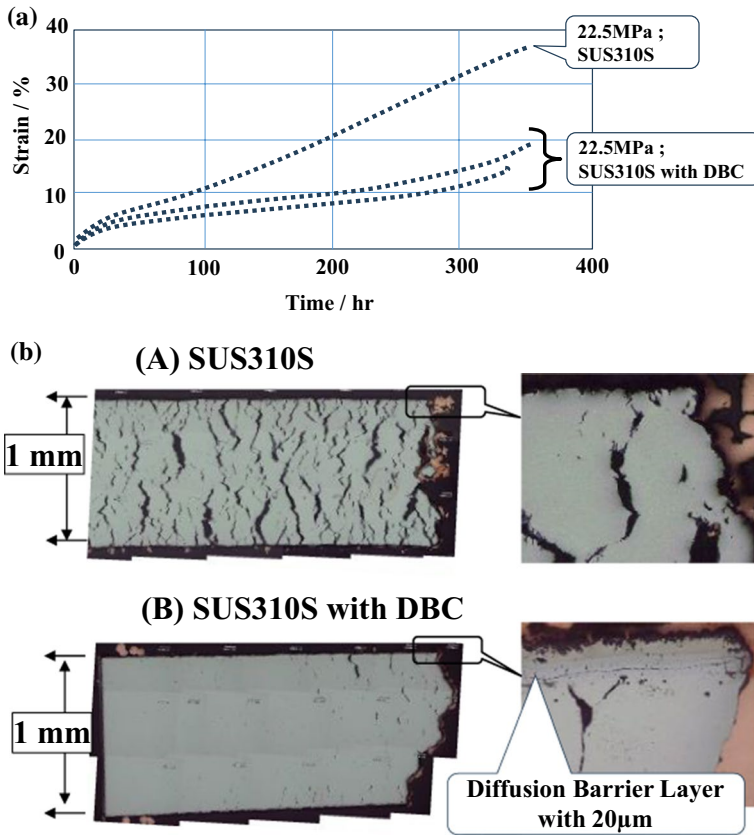


Fig. 9 a Creep curves of SUS310S with and without DBC, b Cross-sectional microstructures of SUS310S with and without DBC after creep-tests

proceeded rapidly from the initial stage, as shown in Fig. 9a, while it was found the creep deformation rate of SUS310 with DBC was small. However, little difference was observed in the fracture time.

Figure 9b shows the cross-sectional microstructures of Fe–25Cr–20Ni alloy (SUS310S) with or without DBC after creep rupture at about 350 h. It was found that the Re-based DBL with 20 μm thickness is creep-deformed slowly and cracks are small in contrast to a lot of grain boundary sliding observed in the SUS310S.

Peel Resistance of YSZ Layer

A DBC/TBC was formed on a disk-shaped HX alloy, and a thermal cyclic oxidation test (1100 °C; 45 min ⇌ RT; 15 min in air) was performed, and the surface morphologies during cooling process were observed with a camera after

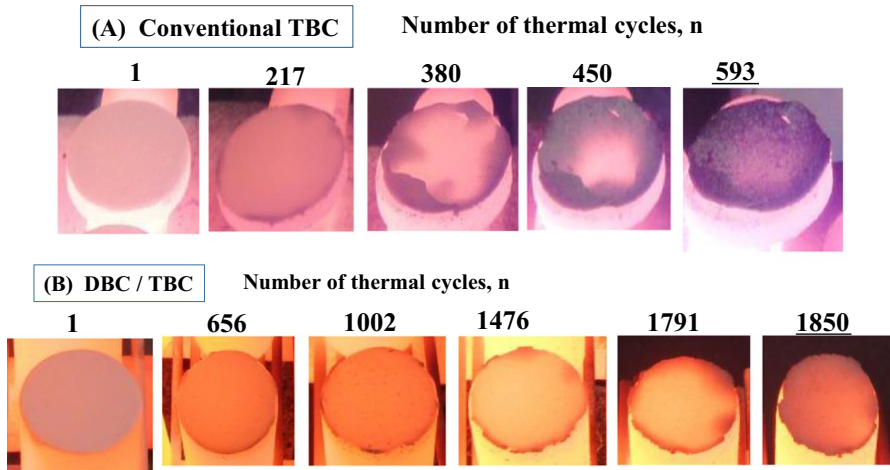


Fig. 10 **A** Top views of YSZ of conventional TBC during cooling from 1100 °C to room temperature in the thermal cycling tests, **B** Top views of YSZ of DBC/TBC during cooling from 1100 °C to room temperature in the thermal cycling tests

pre-determined cycles. For comparison, test pieces with conventional TBC were also tested under the same cyclic oxidation conditions.

For the conventional TBC, as shown in Fig. 10A, peeling of the YSZ layer proceeded from periphery into the substrate, and cracks formed within the YSZ layer, and then the entire YSZ layer peeled off after about 593 cycles.

Meanwhile, as shown in Fig. 10B, the interface detachment of the YSZ layer of the DBC/TBC proceeds slowly from the periphery, but cracks in the YSZ layer and something like that are not observed. It was completely exfoliated after about 1,850 cycles. The exfoliated YSZ layer retained the shape of the disk.

Coatings on Refractory Metals

Self-Maintaining Coating (SMC) System

Refractory metals and their alloys have the highest specific strength at elevated temperatures, while they are used to be suffered from severe degradation due to high temperature oxidation. As an example, a Nb–Hf-based alloy (C103) has the NbSi₂ coating to form protective SiO₂. Although the NbSi₂ coating has much attention, there are several subjects to be solved. One of them is the formation of non-protective Nb₅Si₃ on the NbSi₂ layer due to selective oxidation of Si.

The SMC system with multi-layer structures as Re (Al, Si)_{1.8}/NbSi₂ on Nb–Hf alloy was prepared by making use of electroplating, slurry, and heat-treatment followed by Si and/or Al pack cementsations. Figure 11a shows the SMC coating structure on Nb–Hf alloy with the distribution of each element. The SMC

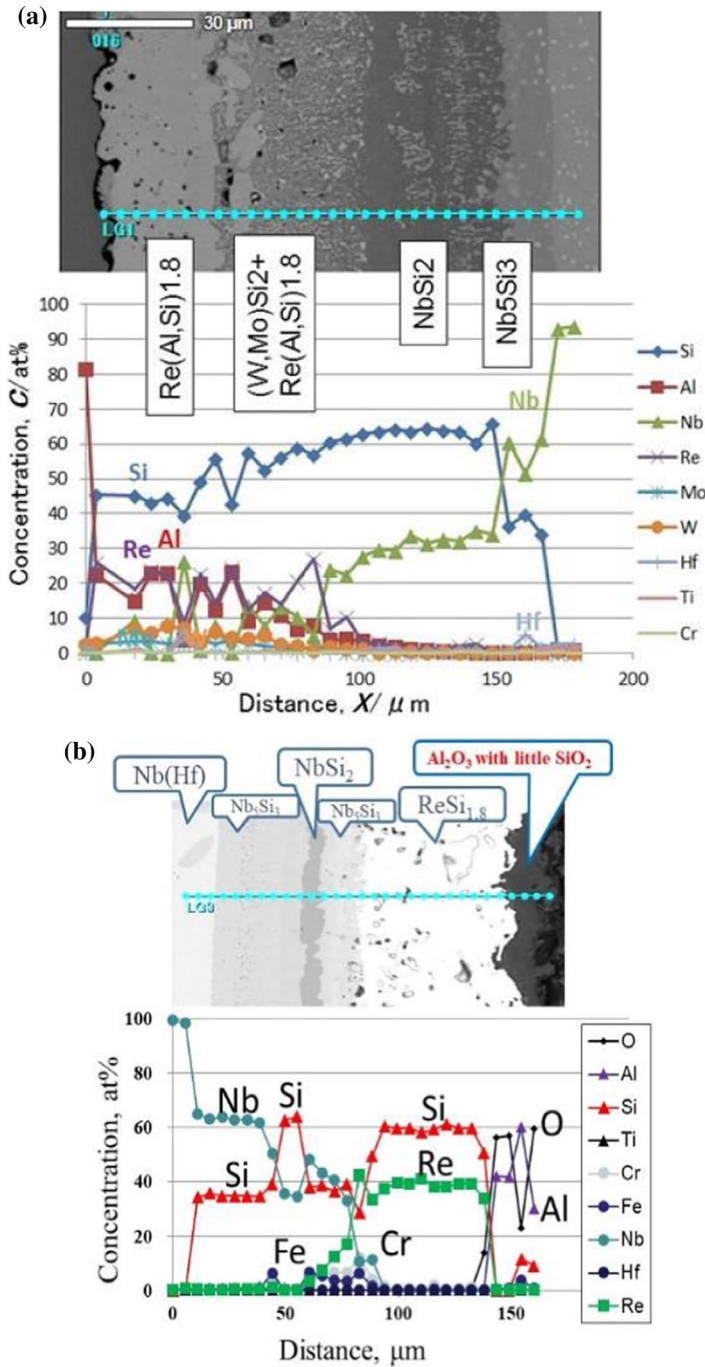


Fig. 11 **a** A Cross-sectional microstructure and concentration profiles across the SMC formed on Nb–Hf alloy, **b** a cross-sectional microstructure and concentration profiles across the Nb–Hf alloy with SMC after oxidation at 1400 °C for 50 h

consisted of $\text{Re}(\text{Al}, \text{Si})_{1.8}$ and NbSi_2 layers, and the $\text{Re}(\text{Al}, \text{Si})_{1.8}$ in the outermost layer varies with the $\text{Re}/\text{Al}/\text{Si}$ concentration ratio.

After oxidation at 1400 °C for 50 h in air, the cross-sectional structure and the concentration of each element are shown in Fig. 11b. It was found from this result that a protective Al_2O_3 film is formed and $\text{Re}(\text{Al}, \text{Si})_{1.8}$ maintains the same crystal structure, while the Si concentration increases up to $\text{ReSi}_{1.8}$. At the same time, NbSi_2 changes to Nb_5Si_3 . Oxidation of $\text{Re}(\text{Al}, \text{Si})_{1.8}$ forms Al_2O_3 via reaction $2\text{Al} + (3/2) \text{O}_2 = \text{Al}_2\text{O}_3$. NbSi_2 decomposes into $\text{Nb}_5\text{Si}_3 + \text{Si}$ and Si will enter into $\text{Re}(\text{Al}, \text{Si})_{1.8}$ to form $\text{ReSi}_{1.8}$.

SMC System with Re (Al, Si, Cr) Layer

The SMC system with the $\text{Re}(\text{Al}, \text{Si})_{1.8}$ layer was modified with addition of Cr to form $\text{Re}(\text{Al}, \text{Si}, \text{Cr}, \text{Nb})_{1.8}$. As shown in Fig. 12A, the SMC layers of $\text{Re}(\text{Al}, \text{Si}, \text{Cr}, \text{Nb})_{1.8}/\text{NbSi}_2/\text{Nb}_5\text{Si}_3$ are in similarity with those in Fig. 11A, except a formation of a mixture of Al_2O_3 and $\text{ReSi}_{1.8}$ at the outer layer (A).

After oxidation at 1400 °C for 40 h the Cr(Nb)-silicide layer (B) in Fig. 12B was formed between $\text{Re}(\text{Si}, \text{Al})_{1.8}$ layer and NbSi_2 layer, accompanied with a growth of an Al_2O_3 in the outermost layer (A). It could be concluded that during high temperature oxidation Cr in the $\text{Re}(\text{Al}, \text{Si}, \text{Cr})_{1.8}$ moved toward NbSi_2 to form Cr(Nb)-silicides, while Al formed Al_2O_3 and Si entered into $\text{Re}(\text{Si}, \text{Al})_{1.8}$ layer from the NbSi_2 layer.

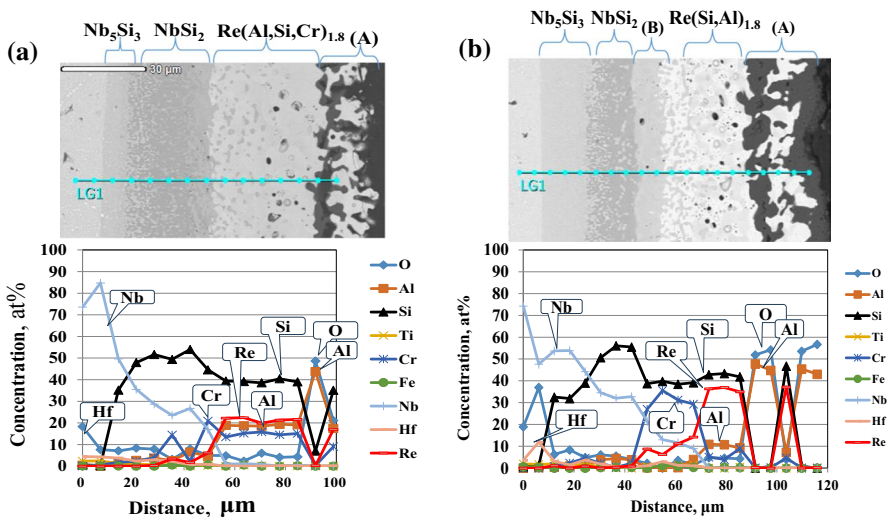


Fig. 12 Cross-sectional microstructures of SMC system formed on Nb–Hf alloy. **A** as-formed and **B** after oxidation at 1400 °C for 40 h in air

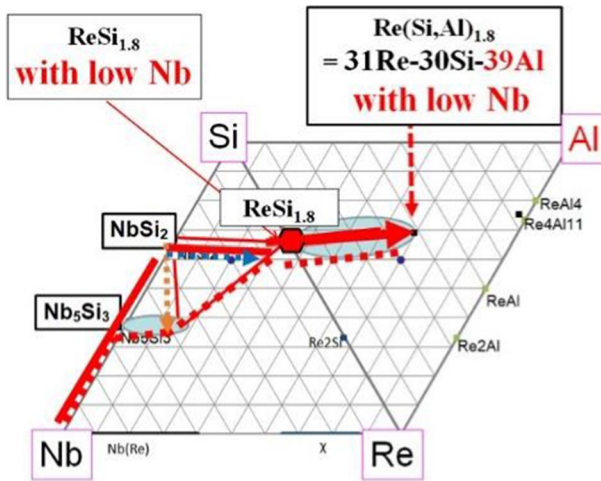
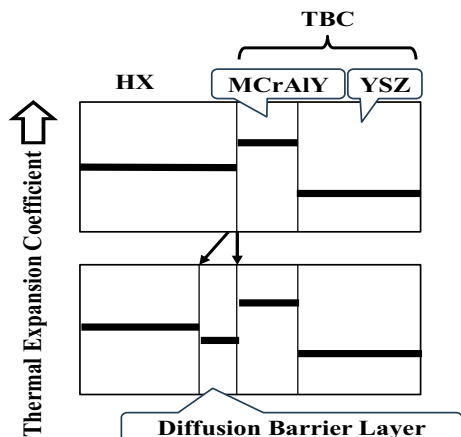


Fig. 13 Composition paths on Nb–Re–Si and Re–Al–Si phase diagrams

Composition Paths

When the composition paths of the SMC with Re (Al, Si)_{1.8} are plotted on the phase diagram in Fig. 13, at the stage of forming Re (Al, Si)_{1.8} the concentration of each element changes along the solid line on the upper side (Si side) of the phase diagram, and in the process of high-temperature oxidation they move along dotted lines on the lower side (Re and Nb).

Fig. 14 Changes in linear expansion coefficients of each layer in alloy substrate (HX) / TBC with and without diffusion barrier layer



Effect of DBL on Peel Resistance of YSZ Layer

As shown in Section "[Peel Resistance of YSZ Layer](#)," it was clarified that the exfoliation resistance of the YSZ (top layer) of the TBC is greatly improved by DBC/TBC. There are also differences in the peeling behavior (delamination and cracking) of the YSZ layer. The exfoliation behavior of the YSZ layer of DBC/TBC and conventional TBC may be controlled by several factors. One of them is the so-called thermal grown oxide (TGO) formed between the YSZ layer and the bond layer (MCrAlY or β -NiAl). The other one seems to be as follows. The author proposed the change in the coefficient of linear expansion due to inserting DBL between the alloy substrate and TBC layer, as shown in Fig. 14.

During the cooling process of thermal cycling, a large tensile stress is generated in the periphery YSZ layer in the alloy substrate/TBC, which promotes cracking of YSZ. While the tensile stress generated in the YSZ layer can be greatly reduced by inserting DBL with low linear expansion coefficients.

The similar arrangement of thermal expansion coefficients has been adopted for the alloy/Si₃N₄ ceramic joints for the ceramic turbo charger rotors, in which an intermediate (Ni/W/Ni) layer was inserted between alloy substrate and Si₃N₄ ceramics. It could be assumed that W layer plays a similar role to DBL as Re, W, and Cr in the DBC system, because of their low expansion coefficients.

Conclusions

This report, focusing on recent progress of the DBC system developed has shown that appropriately designed DBC system improve not only oxidation resistance but also the mechanical properties (creep and fatigue) of alloy substrates and the peel resistance of YSZ. Furthermore, at extreme high temperatures the thermodynamic stability of the alloy plus coating assemblages should be taken into account in addition to kinetic factors, as demonstrated it by the SMC system.

In much of earlier fundamental works, mechanical properties and high-temperature corrosion/protection have been investigated independently. Although elements such as Al, Cr and Si are desirable for the oxidation resistance they provide, their adverse effects on alloy mechanical properties limits their use. The well-known solution is to concentrate these elements in coating, but the coatings must be formulated to be both kinetically and thermodynamically stable during service.

In the design of the oxidation-resistant coating, it is desirable to establish a suitable construction method that takes into account not only oxidation resistance but also structural stability, stress, and mechanical characteristics of the alloy base material. When considering changes in the service environment of materials, it is desirable to develop methods that solve simultaneously the problems of mechanical properties and high-temperature corrosion and protection.

Acknowledgements The first author expressed his deepest appreciation for the proposed DBC and SMC systems, which were the result of a large number of collaborators. Theoretical understanding and explanation on DBC and SMC and their combination are beyond the scope of the authors, and the authors look forward to the efforts which will be made by those who are interested in this report. It is a great pleasure to contribute to the 80th anniversary special issue of the esteemed Professor David Young.

Author contributions TN proposed the project and prepared this paper. YK performed experimental works. TN observed and analyzed the specimens MA performed chemical analyses and prepared figures. All authors reviewed the manuscript.

Declarations

Competing interests The authors declare no competing interests.

Open Access This article is licensed under a Creative Commons Attribution 4.0 International License, which permits use, sharing, adaptation, distribution and reproduction in any medium or format, as long as you give appropriate credit to the original author(s) and the source, provide a link to the Creative Commons licence, and indicate if changes were made. The images or other third party material in this article are included in the article's Creative Commons licence, unless indicated otherwise in a credit line to the material. If material is not included in the article's Creative Commons licence and your intended use is not permitted by statutory regulation or exceeds the permitted use, you will need to obtain permission directly from the copyright holder. To view a copy of this licence, visit <http://creativecommons.org/licenses/by/4.0/>.

References

1. T. Narita, *Japanese Journal of High Temperature Materials* **28**, 2002 (135).
2. T. Narita, T. Izumi, T. Nishimoto, Y. Shibata, K. Z. Thoshin, and S. Hayashi, *Materials Science Forum* **522–523**, 2006 (1).
3. Y. Matsumura, M. Fukumoto, S. Hayashi, A. Kasama, I. Iwanaga, R. Tanaka, and T. Narita, *Oxidation of Metals* **61**, 2004 (105).
4. T. Izumi, T. Yoshioka, and T. Narita, *Journal of the Japan Institute of Metals* **72**, 2008 (728).
5. M. Sakata, S. Hayashi, and T. Narita, *Materials* **47**, 2006 (99).
6. S. Saito, S. Hayashi, Ta. . Narita, Y. Kato, M. Otsuka, M. Ara, and T. Narita, *Materials Transactions* **61**, 2020 (2336).
7. Y. Kato, T. Narita, K. Koseki, M. Aya, and T. Narita, Diffusion and thermal barrier coating systems on Ni-based alloys and their thermal-cyclic oxidation properties, in *Proceedings of ISHOC-2022*, Takamatsu, Japan, pp. 267–270.
8. T. Narita, M. Shoji, Y. Hisamatsu, D. Yoshida, M. Fukumoto, and S. Hayashi, Rhenium coating as a diffusion barrier on a nickel-based superalloy in high temperature oxidation, *High Temperature Corrosion and Protection 2000 Science Reviews*, pp. 351–357.
9. S. Saito, K. Kurokawa, S. Hayashi, T. Takashima, and T. Narita, *Journal of the Japan Institute of Metals* **71**, 2007 (793).
10. Y. Wang, S. Ohnuki, S. Hayashi, T. Yoshioka, M. Hara, and T. Narita, *Materials Transaction JIM* **48**, 2007 (127).
11. S. Saito, K. Kurokawa, S. Hayashi, T. Takashima, and T. Narita, *Journal of the Japan Institute of Metals* **72**, 2008 (132).

Publisher's Note Springer Nature remains neutral with regard to jurisdictional claims in published maps and institutional affiliations.